Journal of the European Ceramic Society **10** (1992) 317–326

Compressive Creep of SiC Whisker-reinforced Alumina

A. H. Swan

Department of Physics, Chalmers University of Technology, S-412 96 Göteborg, Sweden

M. V. Swain

Department of Mechanical Engineering, The University of Sydney, New South Wales 2006, Australia

&

G. L. Dunlop

Department of Mining and Metallurgical Engineering, University of Queensland, St Lucia, Queensland 4067, Australia

(Received 3 September 1991; revised version received 28 November 1991; accepted 15 December 1991)

Abstract

Compressive creep tests of SiC whisker-reinforced Al_2O_3 have been performed in air at temperatures ranging from 1200°C to 1350°C. A creep exponent, n, of ~ 1·5 was obtained, and the activation energy was calculated to be 370 ± 50 kJ/mol. The results are compared to that for creep of a non-reinforced alumina material of similar grain size as well as to the predictions of theoretical models for creep. The microstructure of deformed material has been investigated and related to the creep results. The observations suggest that grain boundary sliding is the dominant creep mechanism. This process was slowed down in the whisker-reinforced Al_2O_3 material by the more extensive shape changes required for the Al_2O_3 grains in order to accommodate grain boundary sliding in the presence of the rigid SiC whiskers. This also resulted in significant cavitation.

Es wurden Kriechversuche mit Druckbeanspruchung an mit SiC-Whiskern verstärktem Al_2O_3 in Luftatmosphäre bei Temperaturen zwischen 1200°C und 1350°C durchgeführt. Der Kriechexponent n ergab sich zu ≈ 1·5 und die Aktivierungsenergie wurde zu 370 ± 50 kJ/mol berechnet. Die Ergebnisse werden einerseits mit Resultaten verglichen, die für nicht verstärkte Aluminiumdioxid-Werkstoffe mit ähnlicher Korngröße erzielt wurden, als auch mit Vorhersagen, die auf theoretischen Kriechmodellen basieren. Das Gefüge des verformten Materials wurde untersucht und im Zusammenhang mit den Ergebnissen der Kriechversuche disku tiert. Die Beobachtungen stützen die Annahme, daß Korngrenzengleitung den dominierenden Kriechmechanismus darstellt. Dieser Prozess fällt in Whisker-verstärktem Material langsamer aus. Der Grund hierzu ist die höhere Formänderung, die Al_2O_3-Körner beim Vorliegen der wenig verformbaren SiC-Whisker erfahren müssten, um Korngrenzengleitung zu ermöglichen. Dies führt ebenfalls zu einer signifikanten Kavitation.

Des tests de fluage par compression d'Al_2O_3 renforcée par des wiskers de SiC ont été pratiqués à l'air et à des températures variant entre 1200°C et 1350°C. Un exposant à la contrainte, n, de ~ 1·5 a été obtenu, et une énergie d'activation de 370 ± 50 kJ/mol a été calculée. Les résultats sont comparés à ceux du fluage de l'alumine non renforcée avec une taille de grain similaire, et aux prédictions des modèles théoriques de fluage. La microstructure d'un matériau déformé a été étudiée et mise en relation avec les résultats du fluage. Les observations suggèrent que le glissement au joint de grain est le mécanisme dominant du fluage. Ce processus est ralenti dans l'alumine renforcée, par les changements de forme plus importants des grains d'Al_2O_3 pour permettre le glissement au joint de grain en présence des wiskers rigides de SiC. Ceci se traduit aussi par une importante cavitation.

1 Introduction

This paper is concerned with the high-temperature creep behaviour of alumina reinforced with SiC

Journal of the European Ceramic Society 0955-2219/92/$5.00

whiskers. It has previously been shown that the fracture toughness and the thermal shock resistance of alumina is significantly improved by the addition of whiskers.[1,2]

The creep strength of Al_2O_3 is also improved by the presence of SiC whiskers and therefore there has been a considerable number of investigations of the creep behaviour of this type of material in recent years. Initial work carried out using four-point bending creep tests suggested that the stress exponent for the creep rate was in the range $n = 4$–6[3–7] but considerably lower values have also been reported.[8] More recent experiments have suggested that bimodal creep behaviour occurs with $n = 1$–2 at low stresses with values of n up to 7 or 8 at high stresses.[9–11] The latter values in ceramics are typical when cavitation and crack generation becomes significant.[12–14]

All of the aforementioned investigations were performed using four-point bending. The analysis for bending creep is complex, since both compressive and tensile stresses are present in the material. The creep rate measurements are also sensitive to the method of measurement, and this can result in large errors in the stress exponent. For example, n has been observed to vary from 1 to 4·6 for a 96% alumina material, depending upon the method of measurement.[15] Furthermore, the strength and creep rate are strongly influenced by the surface tensile properties of the specimens. It has been shown[14] that growth of surface cracks can result in a creep exponent of ~ 2 or higher when the growth rate of microcracks obeys a power-law dependence on the local normal stress. The presence of creep cracks on the tensile surface of crept SiC whisker-reinforced Al_2O_3 has in fact been observed.[7,8]

An investigation of the compressive creep behaviour of SiC whisker-reinforced Al_2O_3 at temperatures between 1200°C and 1500°C gave values of n between 1·2 and 1·8 with an activation energy of 620 ± 100 kJ/mol.[16] These results suggest that the method of creep testing is significant when determining creep parameters of this type. Another compression creep experiment has recently been published,[17] which also studies the effect of ambient atmosphere. The stress exponent was found to be ~ 1 at 1200°C and ~ 3 at 1300 and 1400°C in both air and nitrogen, and the activation energy in air was found to change from 270 kJ/mol to 650 kJ/mol at around 1280°C.

Microstructural observations of crept material have been made by several authors. Porter *et al.*[6] found very little cavitation and some dislocation activity, but concluded that the difference in creep rate between different composites was due to a difference in the aspect ratio of whiskers. Other studies have observed an increased amount of intergranular voids and cavities in composite materials[10,11,16,17] and this is sometimes accompanied by decomposition of whiskers due to oxidation.[7,9,16,17] Liu & Majidi[7] found tensile surface creep cracks that were preferentially in coarse-grained regions of the composite where the concentration of whiskers was low. Whisker pullout and crack bridging by whiskers were also observed and the cracks tended to be short and relatively blunt. It was concluded that the whiskers seemed to play a role in arresting the growth of cracks. Contrary to other work, Donaldson *et al.*[8] found that the presence of whiskers suppressed cavitation and other damage. An analysis of the creep behaviour, using the theory of Kelly & Street,[18] suggested that stress-dependent sliding at the SiC–alumina interfaces and/or whisker fracture was a likely mechanism that could explain the observed stress exponent.

In the present investigation, the creep behaviour of SiC whisker-reinforced Al_2O_3 was measured using compressive creep testing. The effects of surface cracks and other flaws were thus reduced to a minimum. Cylindrical specimens were used in order to reduce edge effects on the creep rate. The results of the high-temperature mechanical testing are compared with the predictions of theory. The microstructure of deformed samples is described and possible creep mechanisms are discussed from a microstructural point of view.

2 Experimental

The experimental material was a commercially available SiC whisker-reinforced Al_2O_3 ceramic matrix composite containing 30 vol% of SiC whiskers (Advanced Composite Materials Corporation, Greer, SC). The material was characterized using optical microscopy, transmission electron microscopy (Jeol 4000FX 400kV TEM/STEM), scanning electron microscopy and X-ray diffraction.

Cylindrical specimens for compressive creep testing with a diameter of 7·5 mm and a length to diameter ratio of approximately 2:1 were trepanned from the as-received material. The opposite faces were ground parallel to ensure a uniform stress distribution under load. Since the whiskers were preferentially oriented in a plane perpendicular to the direction of hot pressing, specimens were cut with the whiskers oriented either parallel or

perpendicular to the direction of the applied load. Due to the initial dimensions of the sample, the specimens with whiskers perpendicular to the applied load had an aspect ratio ~17% less than 2:1.

The creep tests were performed using an Instron servo-hydraulic testing machine model 1343 equipped with a cylindrical split furnace and $MoSi_2$ heating elements. The applied load was transferred via alumina tubes, alumina–zirconia loading plattens followed by SiC plattens at the specimen. The relative movement between the loading plattens was measured using a sensitive ($\pm 0{\cdot}5\,\mu m$) strain gauge extensometer. The specimens were heated to the test temperature at a rate of 600°C/h and then kept at the testing temperature for 45 min before beginning the creep tests. The compressive creep tests were performed using stresses ranging from 25 MPa to 200 MPa at temperatures between 1200°C and 1350°C. When reasonably steady-state creep conditions had been obtained, the load was held constant for another 30 min before being increased. The time elapsed before steady-state conditions were obtained varied with temperature and load, but was of the order of 1 h. This time increased with decreasing temperature. These times maybe considered short when compared with very long-term creep data. After testing, the specimens were cooled down under a stress of 200 MPa. In some cases, a non-loaded reference specimen was included in order to determine the effect of heat treatment without load upon the microstructure.

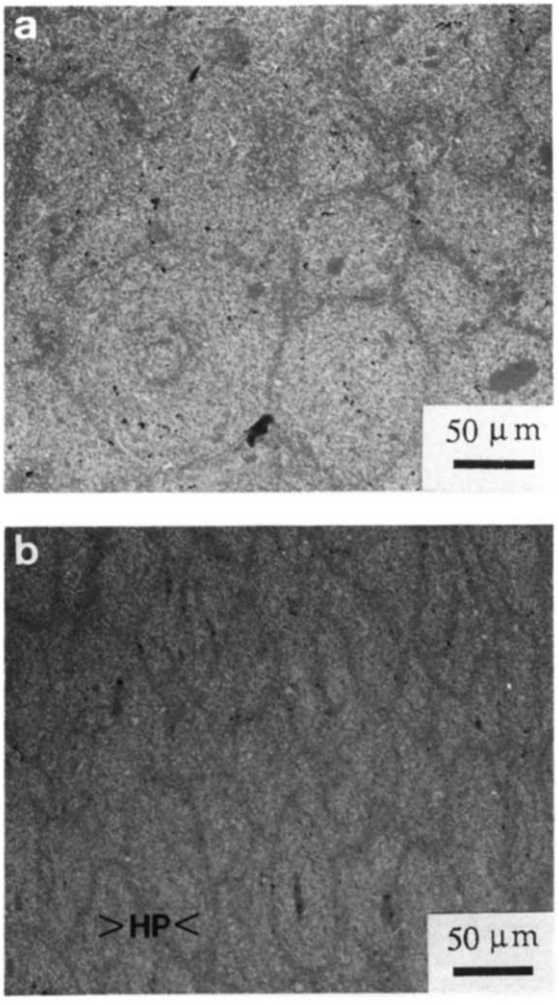

Fig. 1. Granular structure of the as-sintered composite. Optical micrographs (a) of polished surface perpendicular to the hot pressing direction, and (b) surface parallel to hot pressing direction (marked HP).

3 Results

3.1 Microstructure of the composite material

The material appeared to have been fabricated from spray-dried granules that had been hot pressed. The granular structure of the material can be seen in Fig. 1. The granules were lenticular in shape with a maximum dimension of ~100 μm and a thickness in the hot pressing direction of ~40 μm. Preferential orientation of the whiskers in a plane perpendicular to the hot pressing direction can be seen in Fig. 1.

The more detailed microstructure of the as-sintered material is shown in Fig. 2. The grain size of the Al_2O_3 grains was ~1–2 μm, the whisker diameter varied between 0·1 and 1 μm and the aspect ratio of the whiskers was ~10–20. Intergranular films of a glassy phase were present at all whisker–matrix interfaces and some grain boundaries within the Al_2O_3 matrix. They were generally less than 1 nm in thickness. No large intergranular glassy pockets were observed in the as-sintered material. The amorphous films were too thin to allow quantitative EDX analysis; however, qualitative measurements indicated that the film was rich in Si and contained some Ca. The Ca may have come from whisker impurities[19] and the Si from silica-rich layers on the whisker or from low concentrations of silica in the alumina matrix material. The grain size seemed to have been limited by the space available between the whiskers. Some small pores were observed at multigrain junctions and at whisker–matrix interfaces (Fig. 2).

3.2 Creep testing

The dependence of creep rate upon stress was determined by successively increasing the applied load on a single specimen and measuring the creep rate after ~1 h at each value of the applied stress. Extended tests showed that the creep rate continually decreased for longer periods of time (see Fig. 3) and so the creep rates determined after just 1 h at a

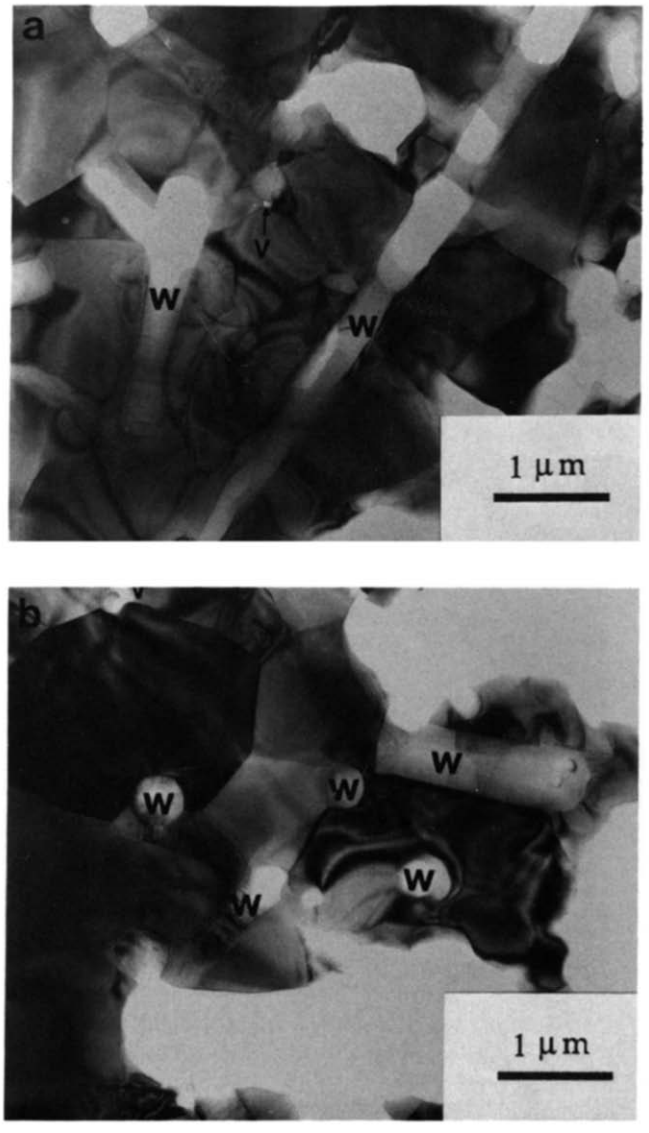

Fig. 2. Microstructure of the as-sintered composite material. The Al_2O_3 grain size appears to be limited by the volume available between the whiskers (W). The interfaces were generally very clean with no large glassy pockets observed. Small voids (V) were sometimes found at multiple grain junctions and at whisker/matrix interfaces. TEM bright field.

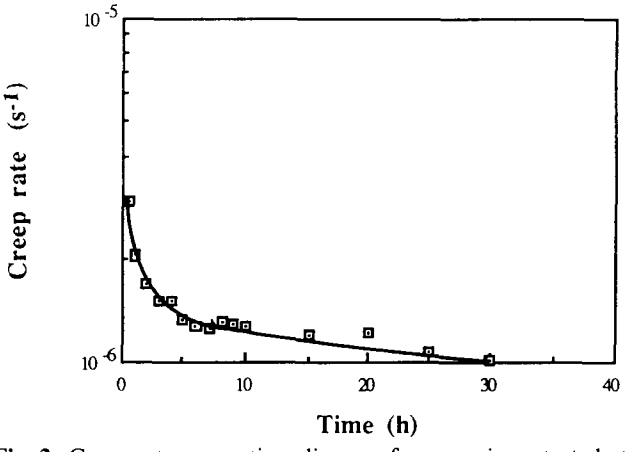

Fig. 3. Creep rate versus time diagram for a specimen tested at 1300°C with a constant compressive stress of 150 MPa. The specimen was cut with the whiskers parallel to the applied load.

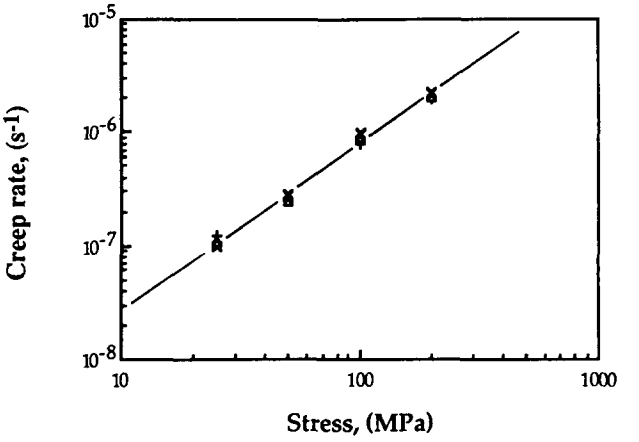

Fig. 4. Creep rate versus stress diagram at 1300°C for specimens with whiskers oriented either parallel or perpendicular to the load. Since the length, l_0 of the perpendicular specimen was 17% shorter than the parallel specimen, a third shortened specimen was tested for comparison. The creep rate was not influenced by the whisker orientation, nor by the small change in l_0. +, Parallel/long; ×, parallel/short; Δ, perpendicular/short.

particular applied load were somewhat faster than a true secondary creep rate. The effect upon the value of the stress exponent, n, was, however, small with an estimated error limit of 0·1. This is within the existing error limits due to misalignment, stress concentrations and non-parallel surfaces.

Creep specimens were cut with the whiskers both parallel and perpendicular to the direction of the applied load with the initial length, l_0, of the latter specimen being ~17% shorter. In order to determine the effect of l_0, a specimen with whiskers parallel to the loading direction was ground down to the same length as the specimens with whiskers perpendicular to the loading direction and tested at 1300°C. Figure 4 shows the creep results obtained for the specimens with different whisker orientations and different initial lengths. There was no significant variation in the observed creep rate due to the

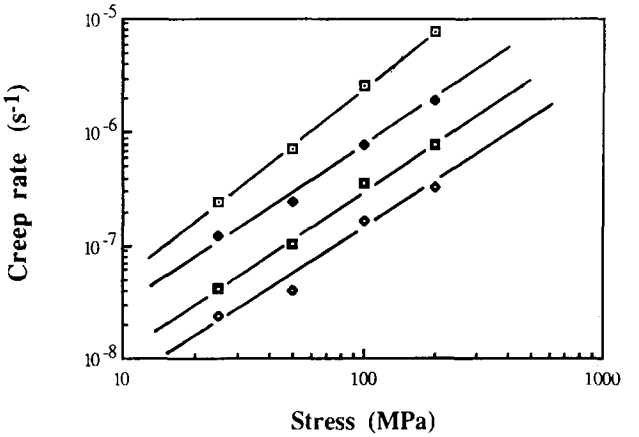

Fig. 5. Creep rate versus stress diagram for specimens with whiskers parallel to the load direction. The stress exponent, n, was found to vary between 1·4 and 1·7. ◆, 1200°C; ■, 1250°C; ◆, 1300°C; ⊡, 1350°C.

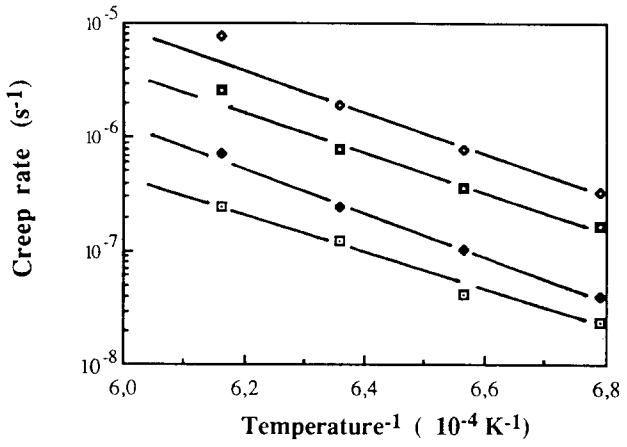

Fig. 6. Arrhenius diagram used to obtain the creep activation energy, Q, for the different stresses applied. Q was found to be 370 ± 50 kJ/mol. ⊡, 25 MPa; ◆, 50 MPa; ■, 100 MPa; ◆, 200 MPa.

whisker orientation, nor was the creep rate sensitive to minor changes in specimen length. Furthermore, Fig. 4 shows that the reproducibility of the data was excellent. However, the specimens with whiskers perpendicular to the applied load were found to chip at both ends during testing. This was not observed for specimens that had the whiskers parallel to the load.

The creep rate data was analysed using the power law equation for steady-state creep,

$$\dot{\varepsilon} = A\sigma^n e^{-Q/RT} \quad (1)$$

where $\dot{\varepsilon}$ is the steady-state creep rate, A is a constant, σ is the applied stress, n is the stress exponent, Q is the creep activation energy, and RT has its usual meaning.

Figure 5 shows the relationship between creep

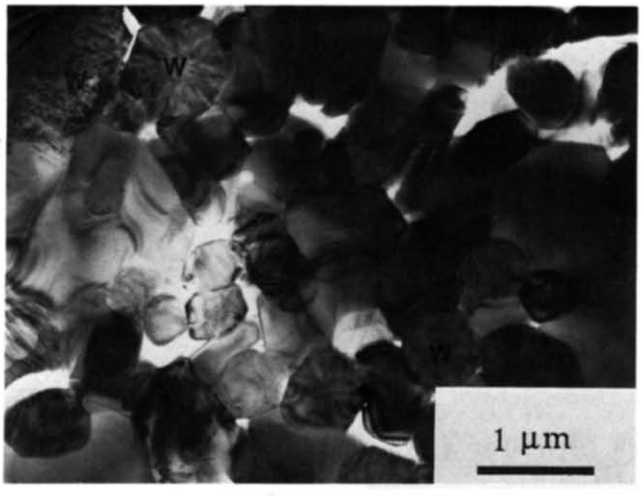

(a)

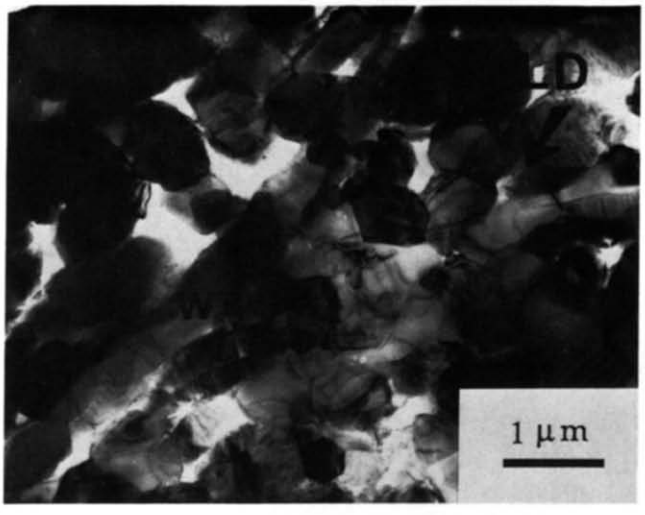

(b)

Fig. 7. Micrographs of the sample deformed ~10% at a constant load of 150 MPa at 1300°C showing the extent of intergranular cavitation due to grain boundary sliding. (a) Specimen cut perpendicular to the load axis, and (b) specimen cut parallel to the load (load direction, LD, as marked). TEM bright field.

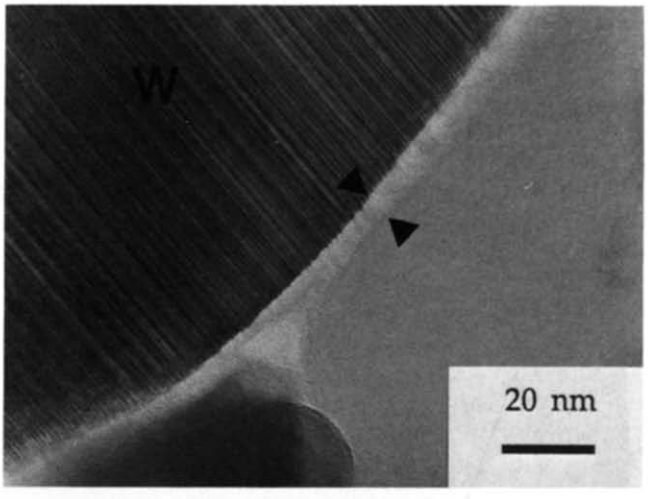

(a)

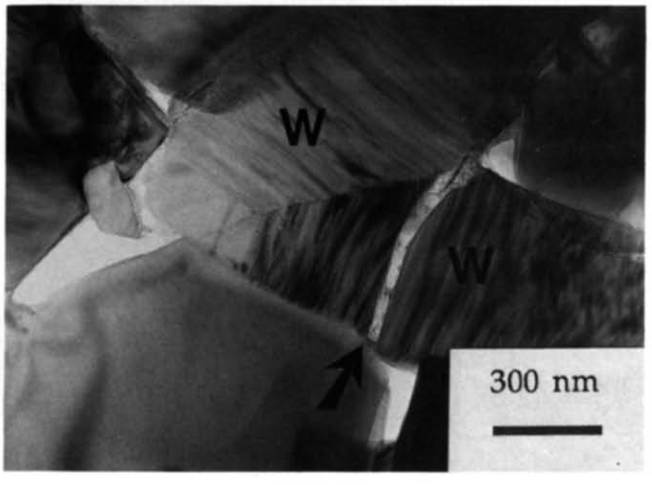

(b)

Fig. 8. Micrographs of (a) glassy interface after whisker oxidation during creep (~1% deformation, 1300°C) and (b) fractured whisker in the same specimen as Fig. 7(b). Note the slight offset of the ends of the whisker and the formation of a glassy phase (arrowed) due to oxidation of the whisker. TEM bright field.

rate and applied stress for specimens with whiskers parallel to the applied load. The creep exponent n was found to vary between 1·4 and 1·7 for the different testing temperature. However, no systematic variation was found. The activation energy, Q, obtained from the Arrhenius plot in Fig. 6, was found to be 370 ± 50 kJ/mol.

3.3 Microstructure of crept specimens

Samples for TEM were cut from the specimen tested at 1300°C that was used to obtain the data in Fig. 3. This specimen had been deformed more than 10% at a constant stress of 150 MPa for ~30 h. The TEM samples were cut both perpendicular and parallel to the direction of the applied load and Fig. 7 shows the microstructure in these specimens. Extensive intergranular cavitation had occurred as a result of grain boundary sliding. The paucity of glassy films between the Al_2O_3 grains in the as-sintered material was also observed in the deformed samples. However, oxidation of SiC whiskers resulted in the formation of a SiO_2-rich glassy phase around the whiskers (Fig. 8) which, in some cases, was found to spread along the grain boundaries into the matrix immediately surrounding the whisker. This glassy film no doubt decreases the viscosity of the grain boundaries and facilitates grain boundary sliding as well as accommodation of grain boundary sliding through increased diffusivity and the ability of the glass to fill voids that would otherwise form at triple junctions. Occasional microcracks were observed as well, extending intergranularly through the specimen (Fig. 9). The general absence of intergranular glassy films at many grain boundaries was inferred from the presence of intergranular dislocation networks in the deformed material. The dislocation density within the alumina grains was also found to increase in the deformed material. However dislocations were only observed in certain limited regions, thus excluding dislocation creep as the rate-controlling mechanism for deformation.

Whisker–matrix interfaces were compared both before and after testing using imaging techniques. In the as-sintered material a micro-roughness of the whisker surfaces was observed due to the stacking sequences of SiC polytypes. The interfaces contained a very thin amorphous film that was only a few monolayers in thickness (Fig. 10(a) and (b)). In the crept material some interfaces had oxidized, resulting in a thicker film of up to ~6 nm along the interface (Fig. 10(c)).

4 Discussion

As shown in Fig. 3, the period of primary transient creep in whisker-reinforced alumina is extensive. This behaviour has been observed to some extent in

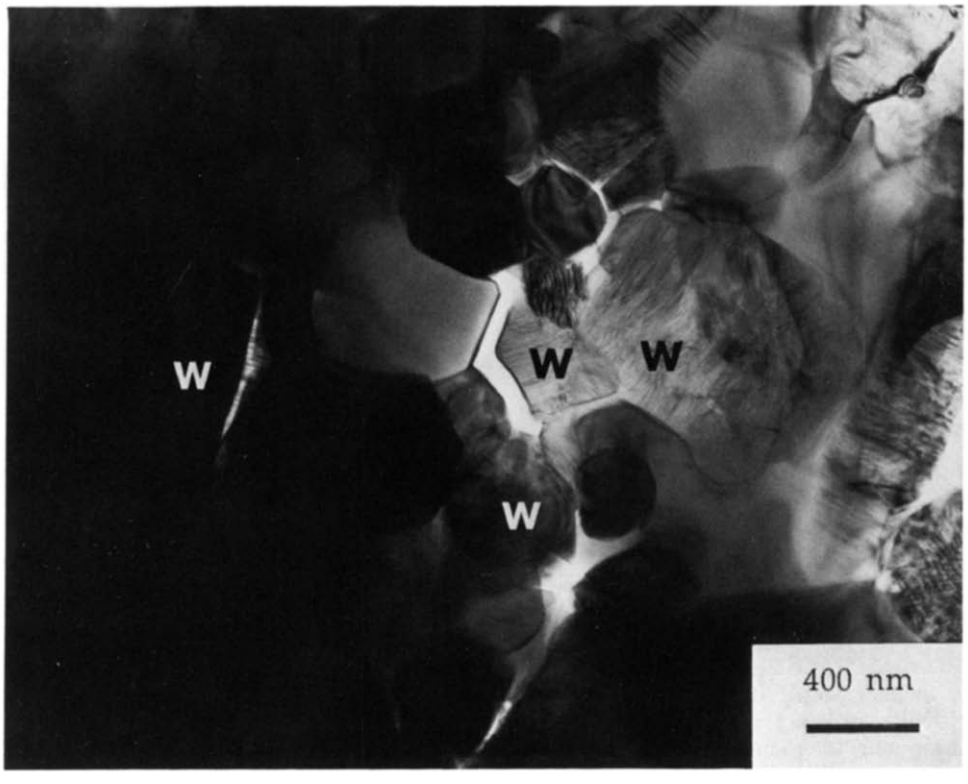

Fig. 9. Micrograph of specimen crept at 1300°C (~10% deformation) showing the formation of an intergranular microcrack due to coalescence of cavities. TEM bright field.

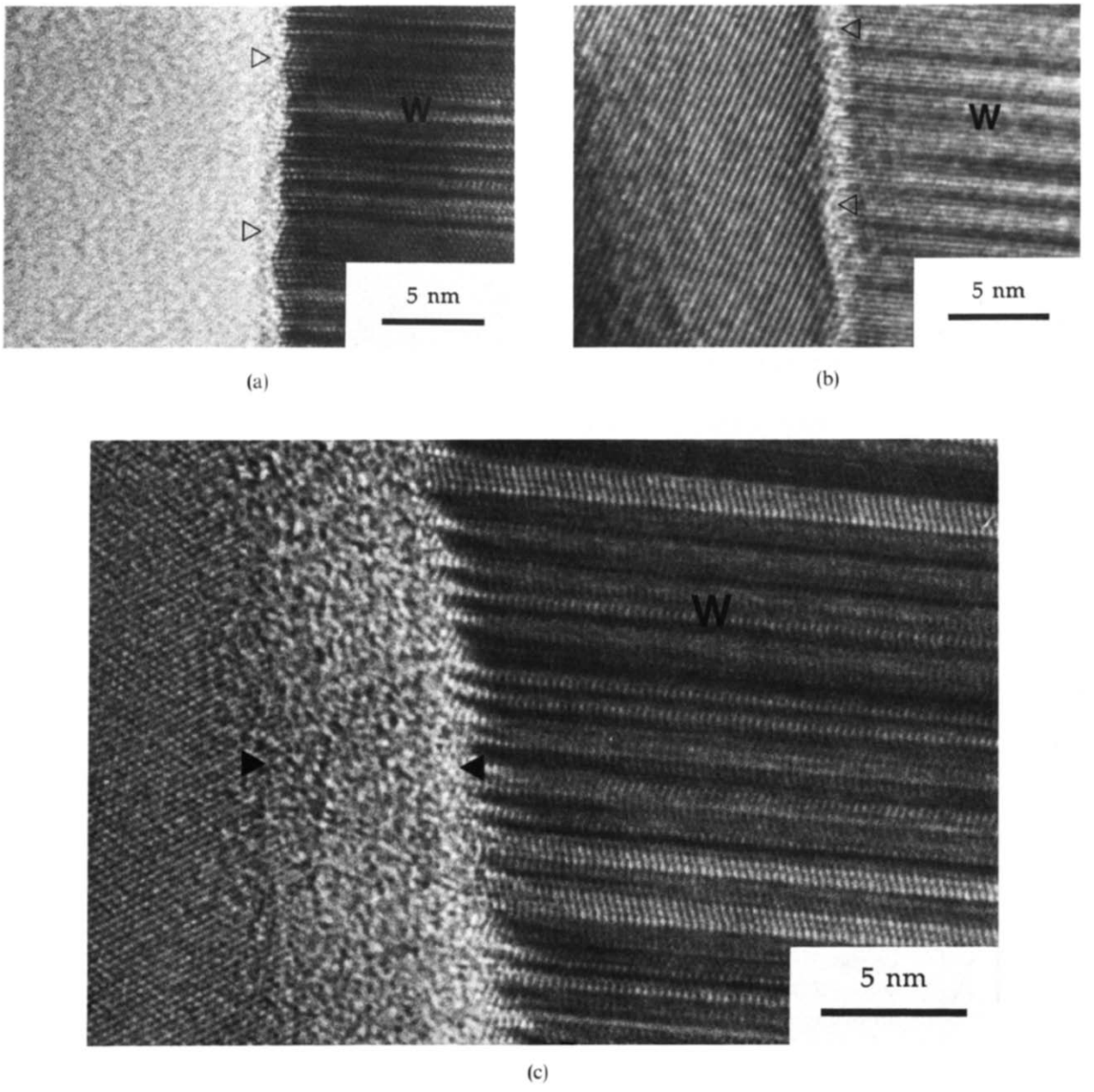

Fig. 10. Lattice images of whisker–matrix interfaces showing (a) and (b) the micro-roughness of the whisker surface with a very thin amorphous film at the interface, and (c) an interface in creep tested material with a thicker glassy film at the interface.

non-reinforced alumina,[20–22] but seems to be more apparent in reinforced materials.[4–6,8,9,11] The creep rate determinations that were made in order to determine the stress dependence of creep rate were generally within the transient region and therefore cannot be considered strictly as secondary creep rates. However, errors that may have been introduced in this way would not have had any significant effect on the stress exponents that were obtained.

The stress exponent ($n = \sim 1{\cdot}5$) found in this investigation was different from many earlier reported results obtained in bending, but was similar to that found in previous work done in compression.[16] No bimodal creep behaviour was observed for the stresses and temperatures used, although bimodal behaviour has been found for a similar material in four-point bending at the same temperatures.[10] The bimodal creep observed in that investigation could have been due to the mode of creep testing, where the rate-controlling mechanism changes to a flaw growth controlled mechanism at higher loads. However, a similar bimodal behaviour has recently been observed in compression creep.[17]

The stress exponent obtained in this investigation is in fact similar to those observed for polycrystalline Al_2O_3 without whisker additions. The activation energy of $Q = 320$–420 kJ/mol is also similar to, but slightly lower than, the activation

energy for cation diffusion in alumina. The activation energy for Al^{3+} lattice diffusion is 478 kJ/mol[23] and for grain boundary diffusion is 418 kJ/mol.[24] This latter value is, however, known to be dependent upon the chemistry of the grain boundaries. In Al_2O_3 the rate-determining creep mechanism is believed to be a diffusional creep process that is either lattice or grain boundary cation diffusion controlled, resulting in a creep exponent of $n = 1$ or interface controlled diffusional creep with $n = 2$.[25]

The possibility of grain coarsening during creep was investigated using scanning electron microscopy of polished samples. No change in grain size was detected in whisker-rich regions, whereas limited growth of the alumina grains was observed in whisker-deficient regions (the areas between the granules). The whiskers thus have the effect of substantially reducing grain growth during creep testing.

The results of the microstructural analysis suggest that the main strain-providing creep deformation mechanism is grain boundary sliding (GBS). The introduction of long, rigid whiskers into the matrix probably slows down the rate of deformation by increasing the amount of shape change that the alumina grains have to undergo for diffusion accommodated GBS. The mean diffusion lengths would be increased by the presence of the whisker, resulting in slower creep rates and also an increased amount of GBS that is not satisfactorily accommodated by grain shape change but which results in cavitation. Evidence of some intragranular dislocation activity was observed in a few Al_2O_3 grains, but the extent of this was too small for it to be rate-determining.

The creep rate of the composite at 1250°C is compared to that of an alumina material tested in compression at 1450°C and adjusted for the difference in temperature (Fig. 11).[21] The material was doped with 500 ppm MgO and had a grain size, d, which varied between 0·8 μm and 3·4 μm depending on sintering time. The stress exponent was found to vary slightly with d, from ~1·2 to ~1·6 for $d = 3{\cdot}4$ to 1·8 μm, respectively, whereas the activation energy, Q, remained constant at ~550 kJ/mol. Equation (1) was used to generate the line in Fig. 11. Since only primary creep was obtained for the alumina material,[21] the creep rate after 10 min of primary creep was used. Flexure creep data of a similar material[25] are included for comparison in Fig. 11, as the data points were obtained at 1259°C (and adjusted for the slight temperature difference). The creep rates were found to be similar and other

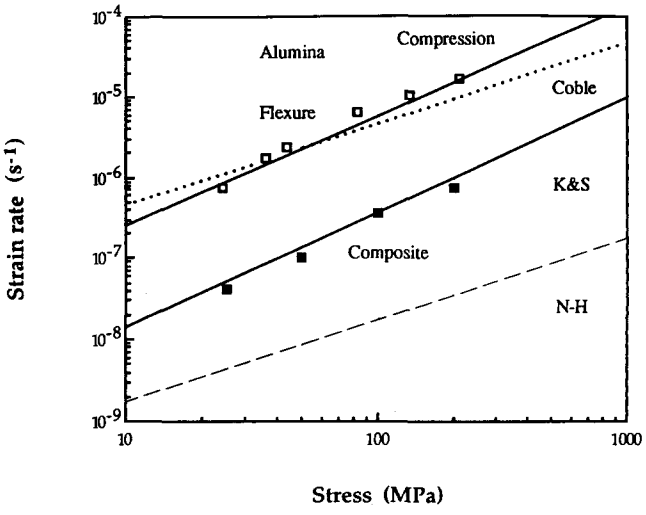

Fig. 11. Creep rate comparison at 1250°C for non-reinforced alumina in compression[21] (–) and flexure[25] (□), the whisker-reinforced alumina investigated here (composite) and the creep rates predicted for Nabarro–Herring creep (N–H) and Coble creep (···). Data for the alumina material were used to model the creep rate of the composite according to the modified theory of Kelly & Street (K&S).[18]

experimental data also give similar creep rates and stress exponents between 1 and 2.[22,26,27] The creep rate of the composite material was found to be about a factor of 20 lower than that for the alumina material.

The data for non-reinforced Al_2O_3 was used to model the creep behaviour of the composite according to the theory of Kelly & Street for rigid short fibres perfectly bonded to the matrix.[18] The assumptions of fibre rigidity and perfect bonding are justified by the very slow creep rate of SiC as compared to alumina and the low glass content of the as-sintered material. As shown in Fig. 11, the creep rates predicted by the Kelly & Street model are very close to the experimental values for the composite material. In the Kelly & Street theory, the creep exponent for the composite is the same as for the matrix material. The $\log \dot{\varepsilon}$–$\log \sigma$ curve is just displaced an amount depending on the aspect ratio and volume fraction of whiskers as well as the stress exponent n.

The model of Kelly & Street was originally developed on the assumption of aligned discontinuous fibres, where the rate of shearing in the matrix is increased, due to the presence of fibres. However, the whiskers in the present material were randomly oriented in two dimensions. A more advanced model has been developed[28] as have also been models which take into account the orientation of the whiskers.[29,30] However, the complexity of the model is then increased without a concomitant gain in accuracy. The model of Kelly & Street is based on tensile creep where no stresses are transferred across

the whisker end surfaces. This is a reasonable assumption for tensile stresses, but is not strictly valid for compressive creep. The analysis should thus be modified in order to include the stress transferred across the whisker end surfaces which should be equal to the stress in the matrix. This modification results in a minor change in the final equation. As has been noted previously[8] calculations have also revealed that a factor in Φ was missing in the original equation. The modified formula can be written as:

$$\sigma_c = \sigma_{m0}\left(\frac{\dot{\varepsilon}_m}{\dot{\varepsilon}_{m0}}\right)^{1/n}\left[\Phi(1-\eta)^{1/n}\left(\frac{l}{d}\right)^{(n+1)/n} V_f + 1\right] \quad (2)$$

where

$$\Phi = (\tfrac{2}{3})^{1/n}\left(\frac{n}{n+1}\right)\left(\frac{n}{2n+1}\right)\left[\left(\frac{2\sqrt{3}}{\pi} V_f\right)^{-1/2} - 1\right]^{-1/n} \quad (3)$$

and is a function dependent on the stress exponent n of the matrix material and the volume fraction of whiskers, V_f. η is the interface sliding factor and $0 < \eta < 1$ ($\eta = 0$ for a perfectly bonded whisker). The dependence of the creep rate upon the stress exponent, whisker volume fraction and whisker aspect ratio ($1/d$) can be seen from eqns (2) and (3). σ_c is the stress required to obtain a certain strain rate $\dot{\varepsilon}_m$ when the creep equation of the matrix material is written as

$$\sigma_m = \sigma_{m0}(\dot{\varepsilon}_m/\dot{\varepsilon}_{m0})^{1/n} \quad (4)$$

As can be expected, this is the equation obtained in eqn (2) when $V_f = 0$. By way of comparison, the original formula of Kelly & Street can be written as[18]

$$\sigma_c = \sigma_{m0}\left(\frac{\dot{\varepsilon}_m}{\dot{\varepsilon}_{m0}}\right)^{1/n}\left[\Phi\left(\frac{l}{d}\right)^{(n+1)/n} V_f + (1 - V_f)\right] \quad (5)$$

where

$$\Phi = (\tfrac{2}{3})^{1/n}\left(\frac{n}{2n+1}\right)\left[\left(\frac{2\sqrt{3}}{\pi} V_f\right)^{-1/2} - 1\right]^{-1/n} \quad (6)$$

For comparison the creep rates predicted for Nabarro–Herring and Coble creep are included in Fig. 11, using these values and an average grain size, d, of 1·6 μm. The creep rate for Nabarro-Herring creep controlled by cation diffusion can be written as[31,32]

$$\dot{\varepsilon} = 40(\Omega_v D_l^+/2kTd^2)\sigma \quad (7)$$

and the rate of Coble creep controlled by cation grain boundary diffusion is[33]

$$\dot{\varepsilon} = (48\Omega_v \delta D_{gb}^+/2kTd^3)\sigma \quad (8)$$

where Ω_v is the molecular volume ($\Omega_v = 4{\cdot}5 \times 10^{-29}$ m^3), k is the Boltzmann constant, σ is the applied stress and T is the absolute temperature.

The orientation of the whiskers was not found to influence the creep rate of the composite material. This unexpected result suggests that the influence of the whiskers might be somewhat different than predicted by the theory of Kelly & Street. There should be another mechanism that operates for whiskers perpendicular to the load direction. The assumption of perfectly bonded whiskers (i.e. $\eta = 0$) could not be justified by the microstructural observations. However, the value of η cannot be precisely determined, which thus increases the uncertainty of the prediction.

The microstructural results for crept material suggest grain boundary sliding as the predominant strain providing creep mechanism. It is suggested that this process is slowed down by the introduction of whiskers, regardless of their orientation. Although the microstructural observations do not directly support the micromechanical model of Kelly & Street, they are certainly compatible with the model.

5 Conclusions

(1) Compressive creep tests of SiC_w-reinforced Al_2O_3 at temperatures ranging from 1200°C to 1350°C resulted in a creep exponent of $n \sim 1{\cdot}5$ and an activation energy for creep of 370 ± 50 MPa.

(2) The observed creep rates for whisker-reinforced material were found to be an order of magnitude lower than that for non-reinforced Al_2O_3 of comparable grain size.

(3) The creep rate was not significantly influenced by the orientation of the whiskers with respect to the applied load.

(4) Microstructural observations suggest that the dominant mechanism of creep deformation is grain boundary sliding. This process was slowed down in the whisker-reinforced material by the more extensive shape changes required for the Al_2O_3 grains in the presence of the rigid SiC whiskers. This also resulted in significant cavitation.

(5) A comparison of the creep rates of composite and alumina materials using a modified version of the analysis by Kelly & Street provided good agreement with the experimental results. However, this analysis is unable to explain the lack of dependence of the creep rate on whisker orientation.

Acknowledgements

Viktor Zelizko of CSIRO, Division of Materials Science and Technology, is thanked for his invaluable help and suggestions during the creep testing. Dr Bill Sinclair of BHP Melbourne Research Laboratories is thanked for supplying the material. Financial support from the Swedish Institute is gratefully acknowledged.

References

1. Becher, P. F. & Wei, G. C., Toughening behaviour in SiC-whisker-reinforced alumina. *J. Am. Ceram. Soc.*, **67** (1984) C-267–C-269.
2. Tiegs, T. N. & Becher, P. F., Thermal shock behavior of an alumina–SiC whisker composite. *J. Am. Ceram. Soc.*, **70** (1987) C-109–C-111.
3. Chokshi, A. H. & Porter, J. R., Creep deformation of an alumina matrix composite reinforced with silicon carbide whiskers. *J. Am. Ceram. Soc.*, **68** (1985) C-144–C-145.
4. Porter, J. R., Lange, F. F. & Chokshi, A. H., Processing and creep performance of SiC-whisker-reinforced Al_2O_3. *Ceram. Bull.*, **66** (1987) 343–7.
5. Xia, K. & Langdon, T. G., The mechanical properties at high temperatures of SiC-whisker-reinforced alumina. In *High Temperature/High Performance Ceramics*, Vol. 120, ed. F. D. Lemkey, S. F. Fishman, A. G. Evans & J. R. Strife. Materials Research Society, Pittsburgh, PA, 1988, pp. 265–70.
6. Porter, J. R., Xia, K. & Langdon, T. G., Microstructural aspects of creep in SiC-whisker-reinforced Al_2O_3. In *Metal & Ceramic Composites: Processing, Modeling & Mechanical Behaviour*, ed. R. B. Bhagat, A. H. Clauer, P. Kumar & A. M. Ritter. The Minerals, Metals & Materials Society, New York, NY, 1990, pp. 381–9.
7. Liu, D. S. & Majidi, A. P., Creep behaviour of SiC_w/Al_2O_3 composites. In *Ceramic Materials & Components for Engines*, American Ceramic Society, Westerville, OH, 1989, pp. 958–67.
8. Donaldson, K. Y., Venkateswaran, A., Hasselman, D. P. H. & Rhodes, J. F., Speculation on the creep behavior of silicon carbide whisker-reinforced alumina. *Ceram. Eng. Sci. Proc.*, **10** (1989) 1191–211.
9. Porter, J. R., Dispersion processing of creep resistant whisker-reinforced ceramic matrix composites. *Mater. Sci. Eng.*, **A107** (1989) 127–32.
10. Lipetzky, P., Nutt, S. R. & Becher, P. F., Creep behavior of an Al_2O_3–SiC Composite. In *High Temperature/High Performance Ceramics*, Vol. 120, ed. F. D. Lemkey, S. F. Fishman, A. G. Evans & J. R. Strife. Materials Research Society, Pittsburgh, PA, 1988, pp. 271–7.
11. Lin, H. T. & Becher, P. F., Creep behavior of a SiC-whisker-reinforced alumina. *J. Am. Ceram. Soc.*, **73** (1990) 1378–81.
12. Dalgleish, B. J., Slamovich, E. B. & Evans, A. G., Duality in the creep rupture of a polycrystalline alumina. *J. Am. Ceram. Soc.*, **68** (1985) 575–81.
13. Thouless, M. D., A review of creep rupture in materials containing an amorphous phase. *Res. Mechanica*, **22** (1987) 213–42.
14. Suresh, S. & Brockenbrough, J. R., A theory for creep by interfacial flaw growth in ceramics and ceramic composites. *Acta Metall. Mater.*, **38** (1990) 55–68.
15. Jakus, K. & Wiederhorn, S. M., Creep deformation of ceramics in four-point bending. *J. Am. Ceram. Soc.*, **71** (1988) 832–6.
16. Arellano-López, A. R., Cumbrera, F. L., Domínguez-Rodríguez, A., Goretta, K. C. & Routbort, J. L., Compressive creep of SiC-whisker-reinforced Al_2O_3. *J. Am. Ceram. Soc.*, **73** (1990) 1297–300.
17. Lipetzky, P., Nutt, S. R., Koester, D. A. & Davis, R. F., Atmospheric effects on compressive creep of SiC-whisker-reinforced alumina. *J. Am. Ceram. Soc.*, **74** (1991) 1240–7.
18. Kelly, A. & Street, K. N., Creep of discontinuous fibre composites II: Theory for the steady-state. *Proc. Roy. Soc. London*, **328** (1972) 283–93.
19. Nutt, S. R., Microstructure and growth model for rice-hull-derived SiC whiskers. *J. Am. Ceram. Soc.*, **71** (1988) 149–56.
20. Chokshi, A. H. & Porter, J. R., High temperature mechanical properties of single-phase alumina. *J. Mater. Sci.*, **21** (1986) 705–10.
21. Gruffel, P. & Carry, C., Strain rate plateau in creep of yttria-doped fine-grained alumina. In *Structural Ceramics, Processing, Microstructure and Properties*, ed. J. J. Bentzen, J. B. Bilde-Sørensen, N. Christansen, A. Horsewell & B. Ralph. Risø National Laboratory, Roskilde, 1990, pp. 305–12.
22. Gruffel, P., Carry, P. & Mocellin, A., Effect of testing conditions on superplastic creep of alumina doped with Ti and Y. In *Science of Ceramics*, Vol. 14, ed. D. Taylor. The Institute of Ceramics, UK, 1988, pp. 587–92.
23. Paladino, A. E. & Kingery, W. D., Aluminium ion diffusion in aluminium oxide. *J. Chem. Phys.*, **37** (1962) 957–62.
24. Cannon, R. M. & Coble, R. L., In *Deformation of Ceramic Materials*, ed. R. C. Bradt & R. E. Tressler. Plenum Press, New York, 1975, pp. 61–100.
25. Cannon, R. M., Rhodes, W. H. & Heuer, A. H., Plastic deformation of fine-grained alumina (Al_2O_3): I. Interface-controlled diffusional creep. *J. Am. Ceram. Soc.*, **63** (1980) 46–53.
26. Venkatachari, K. R. & Raj, R., Superplastic flow in fine-grained alumina. *J. Am. Ceram. Soc.*, **69** (1986) 135–8.
27. Wakai, F., Iga, T. & Nagano, T., Effect of dispersion of ZrO_2 particles on creep of fine-grained Al_2O_3. *J. Ceram. Soc. Jpn*, **96** (1988) 1206–9.
28. Pachalis, J. R., Kim, J. & Chou T. W., Modeling of creep of aligned short-fiber-reinforced ceramic composites. *Comp. Sci. Technol.*, **37** (1990) 329–46.
29. Wang, Y. R. & Chou T. W., Analytical modeling of elevated temperature mechanical behavior of ceramic matrix composites. In *Ceramic Materials & Components for Engines*, American Ceramic Society, Westerville, OH, 1989, pp. 673–82.
30. Wang, Y. R., Liu, D. S., Majidi, A. P. & Chou T. W., Creep characterization of short-fiber-reinforced ceramic composites. *Ceram. Eng. Sci. Proc.*, **10** (1989) 1154–63.
31. Nabarro, F. R. N., Deformation of crystals by the motion of single ions. In *Report of a Conference on the Strength of Solids*. The Physical Society, London, 1948, pp. 75–90.
32. Herring, C., Diffusional viscosity of a polycrystalline solid. *J. Appl. Phys.*, **21** (1950) 437–45.
33. Coble, R. L., Model for boundary diffusion controlled creep in polycrystalline materials. *J. Appl. Phys.*, **34** (1963) 1679–82.